Tissue physical property of the harbor porpoise *Phocoena phocoena* for investigation of the sound emission process

Mika Kuroda

Hokkaido University, 3-1-1, Minato-cho Hakodate, Hokkaido, 041-8611, Japan

Motoki Sasaki, Kazutaka Yamada

Obihiro University of Agriculture and Veterinary Medicine, Nishi 2-11, Inada-cho, Obihiro, Hokkaido, 080-8555, Japan

Nobuhiro Miki

Future University Hakodate, 116-2, Kamedanakano-cho Hakodate, Hokkaido, 041-8655, Japan

Takashi Matsuishi

Hokkaido University, 3-1-1, Minato-cho Hakodate, Hokkaido, 041-8611, Japan

RUNNING TITLE

Phocoena phocoena sound emission

ABSTRACT

The process by which sound is propagated in the head of a toothed whale is still a subject of discussion. Investigating the distribution of acoustic impedance calculated by density and Young's modulus is effective for quantitative comprehension

because acoustic impedance determines the reflection coefficient of a sound wave. However, the sound propagation process of the toothed whale has been mainly examined by either anatomical techniques or the measurement of density or sound velocity. In the current study, the acoustic impedance of head tissue of harbor porpoise was measured. Results of this study should be a helpful information for further discussion about the relationship between the structure of sound-producing organ and clicks property. .

PACS number: 43.80.Ka

I. INTRODUCTION

The harbor porpoise (*Phocoena phocoena*) is a kind of small toothed whale widely distributed in the northern hemisphere (Read et al., 1997). As with other toothed whale, the harbor porpoise recognizes surrounding environment using the echo of high frequency ultrasonic pulses called clicks. The producing and propagation process of clicks in forehead is highly complicated, involving various types of organs and tissues (McKenna et al., 2012).

Elucidation of the sound propagation process of the toothed whale could contribute to the improvement of an acoustic detecting device for example a fish-finder. The principle of how dolphins search for prey using clicks with perfect control had been focused on to improve the fish-finder. The improvement of a fish-finder that uses ultrasonic waves resembling dolphin clicks has been promoted to obtain more detailed information about fish, for example fish species and size (Akamatsu et al., 2012; Imaizumi et al., 2008). Clarification of the clicks emission mechanism should give helpful information for the development of a “dolphin sonar” from a biomimetic standpoint.

It has been confirmed that clicks are produced at the phonic lips, which consist of two pairs of balsae (Cranford et al., 1996; Aroyan et al., 1992), and are propagated to

47 the melon. Clicks beam progressively focused by the melon, air sacs, skull, and
48 collagenous connective tissues located in the forehead region (Cranford et al., 1996;
49 Huggenberger et al., 2009) until they are finally emitted into the seawater. Matching of
50 the acoustic impedance to coordinate the soft tissues must be important for efficient
51 sound emission into the seawater, and mechanisms for this have been suggested (Norris
52 and Harvey, 1974). Considerable amount of research as mentioned above has attempted
53 to elucidate the clicks emission process of toothed whales, however, quantitative
54 information about head soft tissue is much less than anatomical information. Because of
55 the lack of quantitative comprehension, the process by which sound is propagated in the
56 head of the toothed whale remains the subject of debate. For one of the few quantitative
57 comprehension, Soldevilla et al. (2005) measured sound velocity using sliced head
58 tissue from a neonatal Cuvier's beaked whale (*Ziphius cavirostris*). This pioneering
59 study focused on the differences in the physical properties of the head tissue of the
60 Cuvier's beaked whale and tried to measure the elasticity of the soft tissue.
61 Thus, it is necessary to understand how the acoustic impedance is distributed
62 and matched among the soft tissues in order to reveal how sound is propagated in the
63 head of the harbor porpoise. To our knowledge, no conventional studies have directly
64 measured acoustic impedance in the head of toothed whales.

In the current study, we developed a procedure to measure the acoustic impedance of the soft tissues of the head, determined the distribution of acoustic impedance in the head, and investigated quantitative information about the process of sound propagation. We believe the results should contribute to the complete clarification of the process by which clicks are propagated in the toothed whale.

II. MATERIALS AND METHODS FOR EXPERIMENTAL MEASUREMENTS

A. Specimen

A female harbor porpoise (SNH12009-1, 129 cm) that was incidentally caught by a large set net at Hakodate, Hokkaido on April 19, 2012 was used. The animal was found by members of the Hokkaido University Cetacean Research Group who were on board the fishing boat for a porpoise bycatch survey. The porpoise died due to suffocation by drowning because she was buried among fish in the set net and could not control her body position. The body of the porpoise was completely frozen at −20°C within 3 h after confirming her death.

B. Dissection

The forehead of the porpoise, frozen at −20°C, was cut transversely and

serially at a thickness of 15.5 ± 0.89 mm with a saw (Fig. 1). In each slice, the soft tissue was structurally distinguished and categorized into 5 parts by eye, including melon, dense connective tissue, muscular tissue, blubber, and air sacs (Fig. 2). The posterior surface of each slice sample was recorded photographically with a digital camera to record measurement points for Young's modulus. After taking the pictures, a total of 9 slices (A–I) was quickly restored at −20°C.

C. Young's modulus

Young's modulus is defined by the following expression:

$$E = \frac{\sigma}{\varepsilon} \qquad \cdots\cdots\cdots(1)$$

where E(N/m^2) is Young's modulus, σ (N/m^2) is stress, and ε (%) is strain. Young's modulus is estimated as the slope of the regression line of the stress–strain curve (Fig. 3).

To measure Young's modulus, a creep meter (YAMADEN, RE2-33005C) with a column-shaped plunger (φ 5 mm) was used, which is typically used to measure the physical properties of food (Fig. 4). The sliced frozen samples were heated and kept at 25°C on a thermostatic stage until measurement. The tissue load and strain as well as the stress–strain curve were recorded.

The measurements were performed only if the area of the tissue seen in a slice was larger than the area of the plunger; this was performed up to 3 times in each part of the tissue. At the most rostral slice (A) the Young's modulus could not be accurately measured because of small size and the shape of the sample. All measured points (N = 89) were indicated in Fig. 5.

D. Measurements of the image data using computed tomography

Computed tomography (CT) images was used to estimate the density of the measurement points of Young's modulus. Three hundred fifty seven CT images were obtained every 0.5 mm using a multi-slice CT scanner (Asteion TM Super 4107 Edition; Toshiba, Tokyo, Japan) before slicing, after the scan, the CT values (Robb, 1999) were obtained using a specialized workstation (ZioTerm™ 2009; Ziosoft, Tokyo, Japan). A CT value at each measured point of Young's modulus that matched the CT image and the photographs of the sliced head was extracted.

E. Procedure for the calculation of acoustic impedance

Sound speed ($\underline{c}$) and tissue density ($\underline{\rho}$) led to the calculation of the acoustic impedance (Z) using the following equation (2):

$$Z = \rho c \quad \text{.....(2)}$$

Young's modulus (E) and tissue density (ρ) led to the calculation of the sound speed ($\underline{c}$) using the following equation (3):

$$c = \sqrt{\frac{E}{\rho}} \quad \text{.....(3)}$$

Combining these equations, the acoustic impedance is calculated directly from Young's modulus and tissue density as follows;

$$Z = \sqrt{\rho E} \quad \text{.....(4)}$$

The physical properties were plotted at the measuring points of Young's modulus on a three-dimensional reconstructed CT image.

III. EXPERIMENTAL RESULTS

A. Physical properties of tissue in the melon

Figure 5 shows the average density, Young's modulus, and acoustic impedance at each measured point expressed as the length from the tip of the upper lip plotted for the melon, dense connective tissue, blubber, and air sacs. The acoustic impedance of

132 melon was approximately 1608 Pa·s/m at the edge of the rostrum and 283 Pa·s/m close
133 to the phonic lips.The acoustic impedance of 1500 Pa·s/m which matches that of
134 seawater was found by linear interpolation to be 41 mm from the animal's upper lip.
135 Therefore, the clicks were considered to be emitted underwater at the area centering at
136 4cm from the rostrum’s edge. The impedance of the other tissues was less than
137 1000 Pa·s/m.
138
139 **B. Head tissue structure of the harbor porpoise**
140 Figure 6 shows reconstructed three-dimensional CT images of the tissue
141 structures of the forehead, layered in different colors. The dense connective tissue was
142 observed in the rostral part of the forehead under the skin, as if it were surrounding the
143 melon. The frontal part of the melon protruded from a circular aperture, called “emitting
144 surface” hereafter, formed by the dense connective tissue and was located directly under
145 the skin. In the posterior part of the melon, the blubber was laid broadly under the skin,
146 and the muscular tissue and air sacs were arranged in the medial part of the blubber. In
147 this part, however, the dense connective tissue was on the melon and surrounded by
148 muscular tissue.
149

C. Distribution of acoustic impedance

Figure 7 shows the distribution of the acoustic impedance plotted onto the measuring points of Young's modulus. The size of the spheres indicates the relative value of the acoustic impedance. The difference in the acoustic impedance between the melon and other soft tissues gradually increased from the phonic lips to the tip of the melon. In addition, the value of the acoustic impedance at the emitting surface was approximately 1400–1700 Pa·s/m. In this range, the acoustic impedance of seawater (approximately 1500 Pa·s/m) was included and this matching sould be contribute to efficiently emission of clicks.

Figure 8 shows the three-dimensional distribution of the acoustic impedance. The tissues covering the melon had relatively less impedance than the melon. These tissues should play a reflective role and prevent sound from leaking out of the melon.

IV. DISCUSSION

Our experimental results re-examined the possible process by which clicks are propagated in the head of the harbor porpoise by investigating the distribution of the acoustic impedance calculated by density and Young's modulus. In the melon, a continuous increase in the acoustic impedance was observed from the sound source to

168 the tip of upper lip until it was equal to that of the seawater at the emitting surface
169 (Fig. 5). These results support the proposed function for the melon of the harbor
170 porpoise as a tissue to match the acoustic impedance of the seawater, as has been
171 proposed for the bottlenose dolphin (Norris and Harvey, 1974). However, to the best of
172 our knowledge, we are the first to suggest that the acoustic impedance is conducted in a
173 rostral–caudal direction. Furthermore, Harper et al. (2008) examined the role of the
174 rostral muscles inserted into the blubber surrounding the melon. They suggested that
175 contraction of the rostral muscles increases the local stiffness of the blubber, which
176 could change the refraction of the emitted echolocation beam. In our current study, a
177 post-mortem specimen was used, so no contraction of muscle could occur. However, the
178 difference in the acoustic impedance between the melon and the muscle was very small
179 around the source of the sound and gradually increased from there to the rostrum (Fig. 5,
180 Fig. 7). This implies that if contraction of the rostral muscle did not occur at the same
181 moment as when the clicks were produced, the clicks' waves could propagate and be
182 absorbed into the muscle around the source of the sound and be reflected near the
183 rostrum.

184 According to Fig.6, when the acoustic impedance of melon increases by
185 10.6% (x-coordinate: from 57.47mm to 46.05mm), Young's modulus increases by

186 21.8% and the density increases only by 0.5%. From this result, when the acoustic
187 impedance changes, the change rate of Young's modulus would occupy a larger
188 percentages than that of density in condition of the current study.
189 Therefore, Young's modulus should be more focused as an index for the sound
190 propagation process. The process of sound propagation has been studied by measuring
191 sound speed or density changes in head tissue (Soldevilla et al., 2005; McKenna et al.,
192 2012). These precise knowledge has provided significant implications about the
193 distribution of the density and the speed of sound in soft tissue structures, However, the
194 results of the current study suggest that density should not be used alone as an index of
195 sound propagation. Combination of density and Young's modulus should provide better
196 estimation of sound propagation process..
197 The dense connective tissue surrounding the lateral and posterior part of the
198 melon construct the emitting surface (Fig. 6). Analysing a CT image in detail showed
199 that the fiber direction of the connective tissue was perpendicular to the dorsal-caudal
200 direction and that the fibers ran parallel to each other. According to the distribution of
201 the acoustic impedance, clicks are most likely to be emitted from the emitting surface,
202 supporting a previous study (Au et al., 2006). The connective tissue itself should act like
203 a reflector in the head and work to reflect the beam of the clicks into the melon.

Therefore, more attention should be paid to the idea that the connective tissue functions not only to support the melon but also as a kind of acoustic organ.

In addition to melon and other soft tissue discussed in the current study, the air space constructed by air sac and skull would be also play the central role in the sound propagation process (Aroyan et al., 1992). To investigate the clicks propagation process, the acoustical simulation such as finite element model approach (Tao et al., 2008; Cranford et al., 2014; Wei et al., 2014) is conducted. In the model, the physical property of head soft tissue is regarded as fluid which have uniform density and sound velocity. If the more detailed physical property of head soft tissue as measured in this study was applied to the simulation, the boundary condition would be closer to the real head of dolphin. Using detailed physical property of head structure, the advantage of the finite element model which able to process the complex boundaries and fine spatial information would be fully exploited.

V. CONCLUSIONS

In the current study, density and Young's modulus were measured to derive the value of acoustic impedance. Subsequently, the distribution of the measurement values of these three physical properties was investigated. The distribution and the relationships of

physical properties implies that when the change of Young's modulus would occupy a larger percentages against the density in condition of the current study.

Only in the melon, low impedance around the sound source gradually increased and matched with the impedance of the seawater at the emitting surface. The impedance gap between the melon and the other tissues gradually increased from the source of the sound to the emitting surface of the dense connective tissue.

Our results allowed us to estimate the structures that propagate clicks in the acoustic pathway and to estimate how these tissue structures work in the sound propagation system in a porpoise’s head. To reveal the relationship between structure of sound-producing organ and clicks property, further discussion about the detailed function of those soft tissue structures will be necessary. Measuring and comparing the physical property of other small toothed whale which have different clicks frequency, bandwidth and directivity should enable the higher-precision simulation of the clicks propagation process in the head of toothed whales.

ACKNOWLEDGEMENTS

The authors are indebted to Hisanori Nozawa and Koretaro Takahashi for the advice on using the creep meter for measurements. We would also like to thank the

240 Stranding Network Hokkaido and Hokkaido University Cetacean Research Group for
241 supporting our access to the harbor porpoise. This study was carried out in accordance
242 with the National University Corporation Hokkaido University Regulations on Animal
243 Experimentation. Authorization number: 12-0004. This work was supported by JSPS
244 KAKENHI Grant Numbers 26450255 and 25281008.

245

246 **REFERENCES**

247 Akamatsu, T., Imaizumi, T., Abe, K., Nishimori, Y., Wang, Y., Matsuo, I., and Ito, M.,
248 **(2012).** "A broad band dolphin mimetic sonar—inspiration and modification
249 from the nature," J. Acoust. Soc. Am. **131,** 3422-3422.

250 Au, W. W., Kastelein, R. A., Benoit–Bird, K. J., Cranford, T. W., and McKenna, M. F.
251 **(2006).** "Acoustic radiation from the head of echolocating harbor porpoises
252 (*Phocoena phocoena*)," J. Exp. Biol. **209,** 2726-2733.

253 Cranford, T. W., Amundin, M., and Norris, K. S. **(1996).** "Functional morphology and
254 homology in the odontocete nasal complex: implications for sound generation,"
255 J. Morp. **228,** 223-285.

256 Cranford, T. W., Trijoulet, V., Smith, C. R., and Krysl, P. **(2014).** "Validation of a
257 vibroacoustic finite element model using bottlenose dolphin simulations: The

dolphin biosonar beam is focused in stages," Biocoustics **23**, 161–194.

Harper, C. J., McLellan, W. A., Rommel, S. A., Gay, D. M., Dillaman, R. M., and Pabst, D. A., (**2008**). "Morphology of the melon and its tendinous connections to the facial muscles in bottlenose dolphins (*Tursiops truncatus*)" J. Morphol., **269**, 820–839.

Huggenberger, S., Rauschmann, M. A., Vogl, T. J., and Oelschläger, H. H. **(2009).** "Functional morphology of the nasal complex in the harbor porpoise (*Phocoena phocoena* L.)," Anat. Rec. **292,** 902-920.

Imaizumi, T., Furusawa, M., Akamatsu, T., and Yasushi Nishimori, Y., **(2008).** "Measuring the target strength spectra of fish using dolphin-like short broadband sonar signals" J. Acoust. Soc. Am. **124,** 3440.

McKenna, M. F., Cranford, T. W., Berta, A., and Pyenson, N. D. **(2012).** "Morphology of the odontocete melon and its implications for acoustic function," Mar. Mamm. Sci. **28,** 690-713.

Norris, K. S., and Harvey, G. W. **(1974).** "Sound transmission in the porpoise head," J. Acoust. Soc. Am. **56,** 659-664.Read, A. J., Wiepkema, P. R., and Nachtigall, P. E. **(1997).** *The Biology of the Harbor Porpoise* (De Spil Publishers, Woerden, the Netherlands), Chap. 1, pp. 3.

Robb, R. A. **(1999).** *Biomedical imaging, visualization, and analysis* (John Wiley & Sons, Inc. New York, NY, USA), Chap. 2, pp. 33.

Soldevilla, M. S., McKenna, M. F., Wiggins, S. M., Shadwick, R. E., Cranford, T. W., and Hildebrand, J. A. **(2005).** "Cuvier's beaked whale (*Ziphius cavirostris*) head tissues: physical properties and CT imaging," J. Exp. Biol. **208,** 2319-2332.

Tao, C., Jiang, J. J., and Zhang, Y. **(2006).** "Simulation of vocal fold impact pressures with a self-oscillating finite-element model," J. Acoust. Soc. Am. **119**, 3987–3994.

Wei, C., Zhang, Y., and Au, W. W. L. **(2014).** "Simulation of ultrasound beam formation of baiji (*Lipotes vexillifer*) with a finite element model," J. Acoust. Soc. Am. **136**, 423.

FIGURE CAPTIONS

FIG. 1. (A) The head of a harbor porpoise. Broken lines indicate the cutting-plane lines and letters (A–I) were assigned to distinguish each slice. (B) Slices A–I.

FIG. 2. A sliced head of a Dall's porpoise, similar to that of the harbor porpoise. (A) dense connective tissue, (B) melon, (C) blubber, (D) air sacs, and (E) muscular tissue.

FIG. 3. The stress–strain curve of Young's modulus in the melon.

FIG. 4. The measurement of Young's modulus using the creep meter..

FIG. 5. The average density, Young's modulus, and acoustic impedance *versus* length from the rostrum. An image of *Phocoena phocoena* was matched with the horizontal axis. The bold black horizontal line indicates the impedance of seawater.

FIG. 6. A reconstructed computed tomography image of the head of *Phocoena phocoena* from (A) rostral, (B) sagittal, and (C) dorsal. The area enclosed by dotted line is ES, which indicates the emitting surface.

FIG. 7. The distribution of the acoustic impedance in the head of *Phocoena phocoena* from (A) dorsal, (B) rostral, and (C) sagittal. The background figure of reconstructed computed tomography image is identical to FIG. 6.

FIG. 8. The three-dimensional distribution of the acoustic impedance. The size of sphere indicates the impedance value. The background figure of reconstructed computed tomography image is identical to FIG. 6

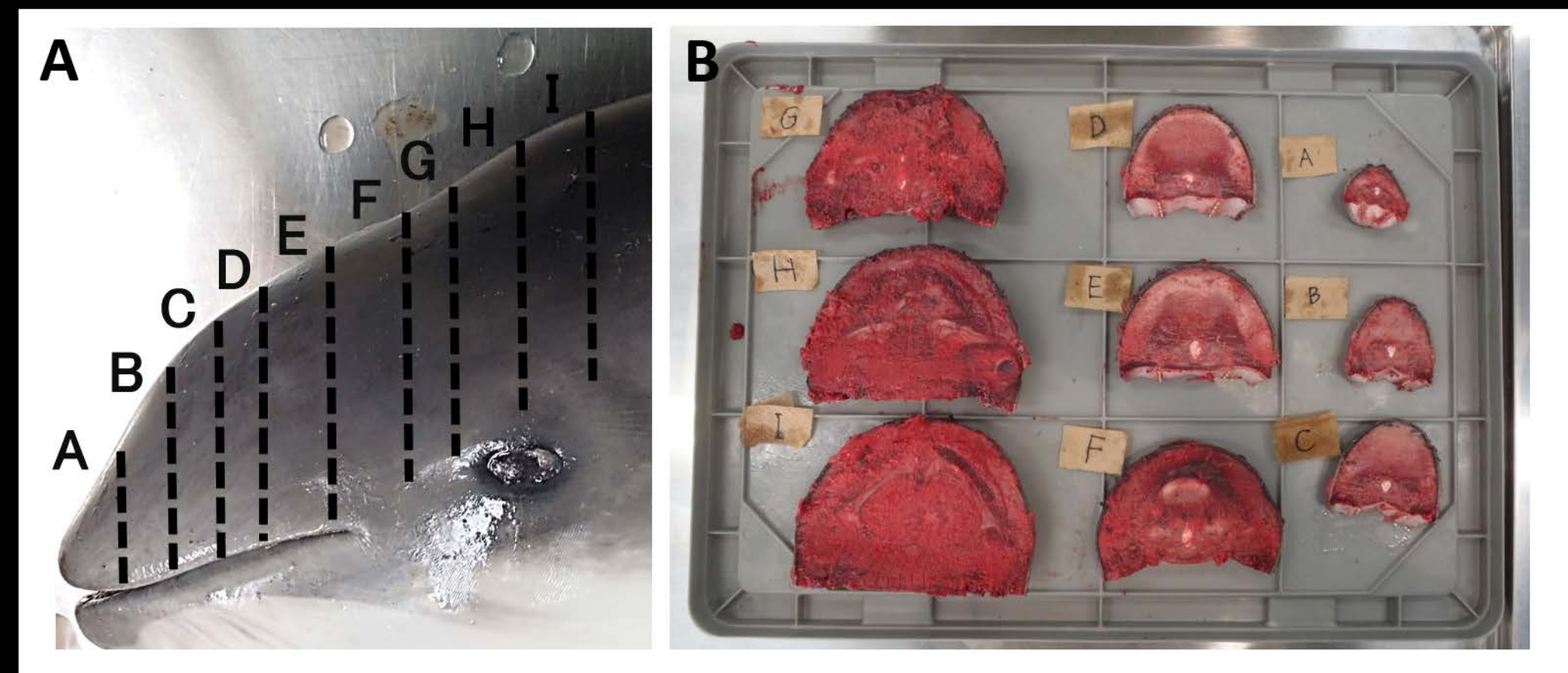
A
A
B
C
D
E
F
G
H
I
B
G
D
A
H
E
B
I
F
C

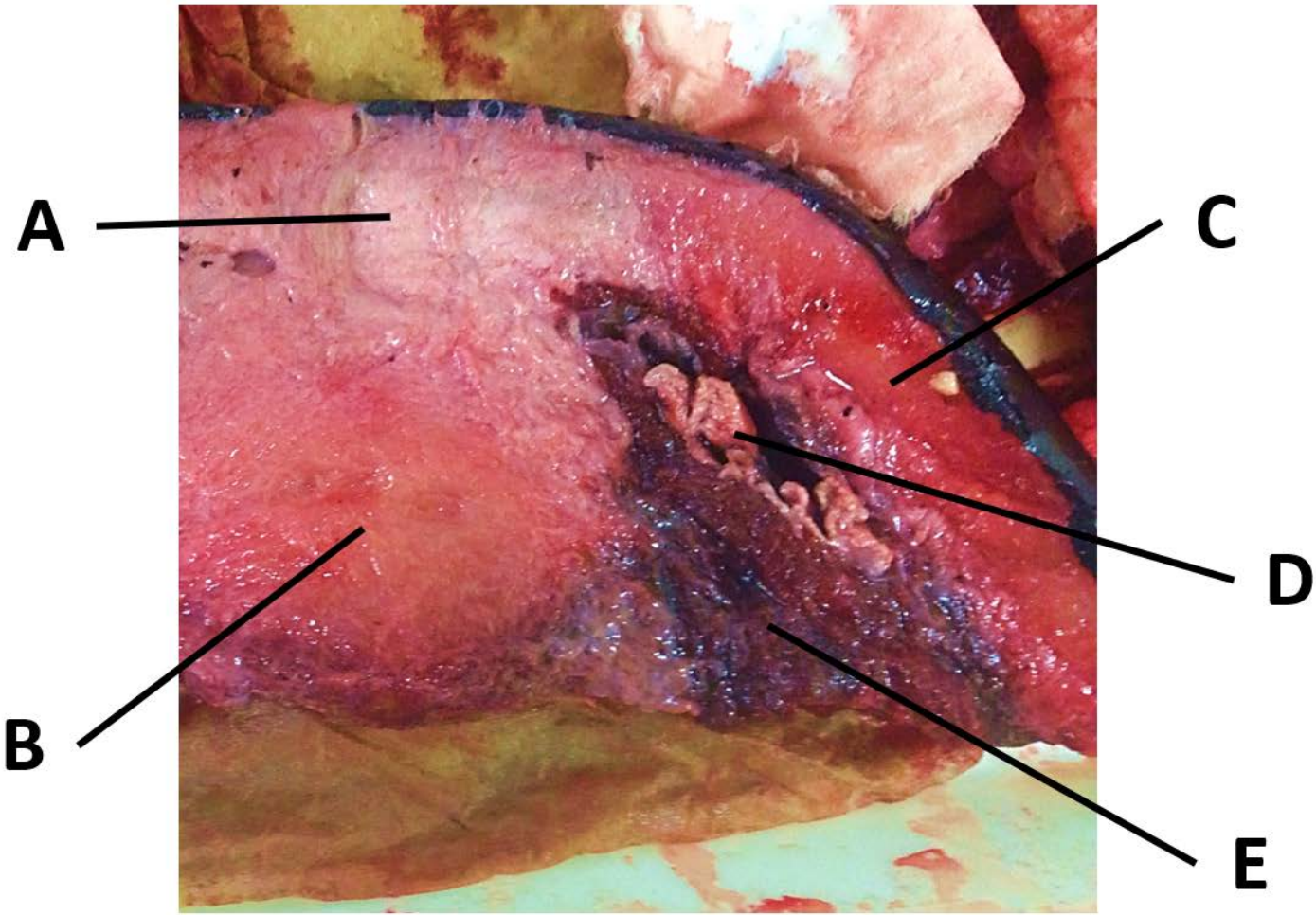
A
B
C
D
E

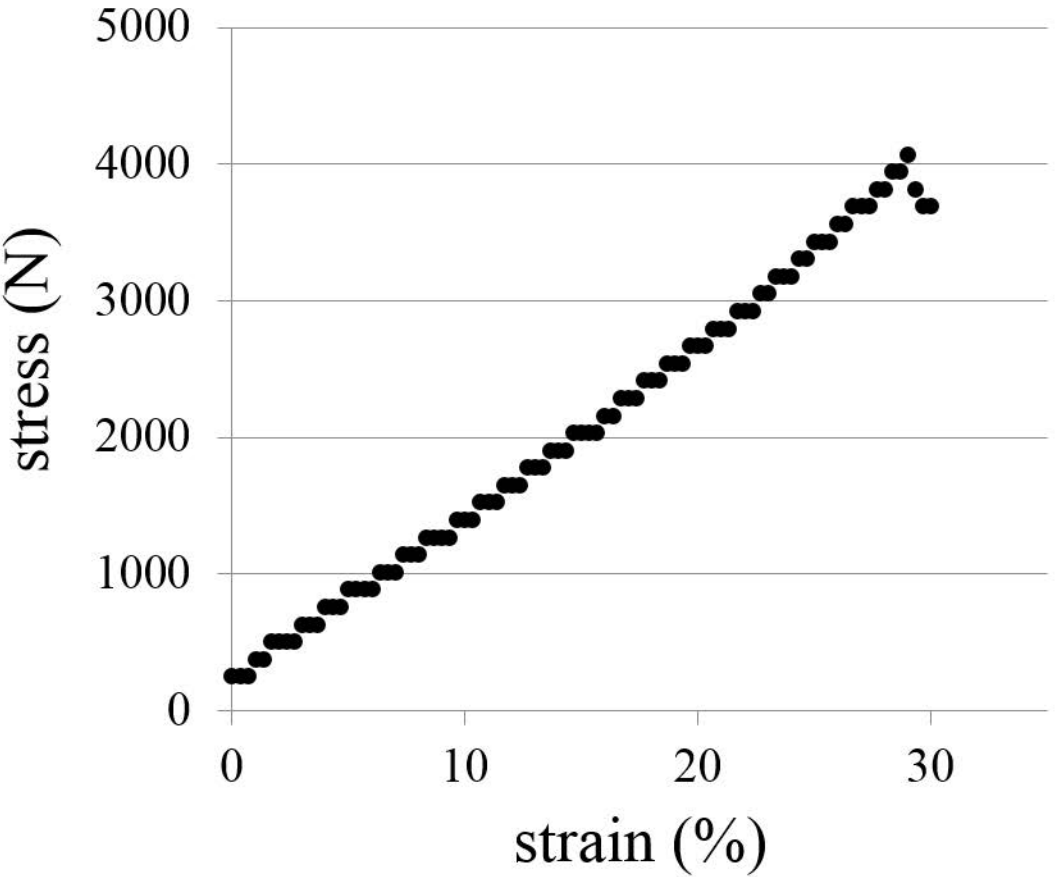
5000
4000
3000
2000
1000
0
stress (N)
0
10
20
30
strain (%)

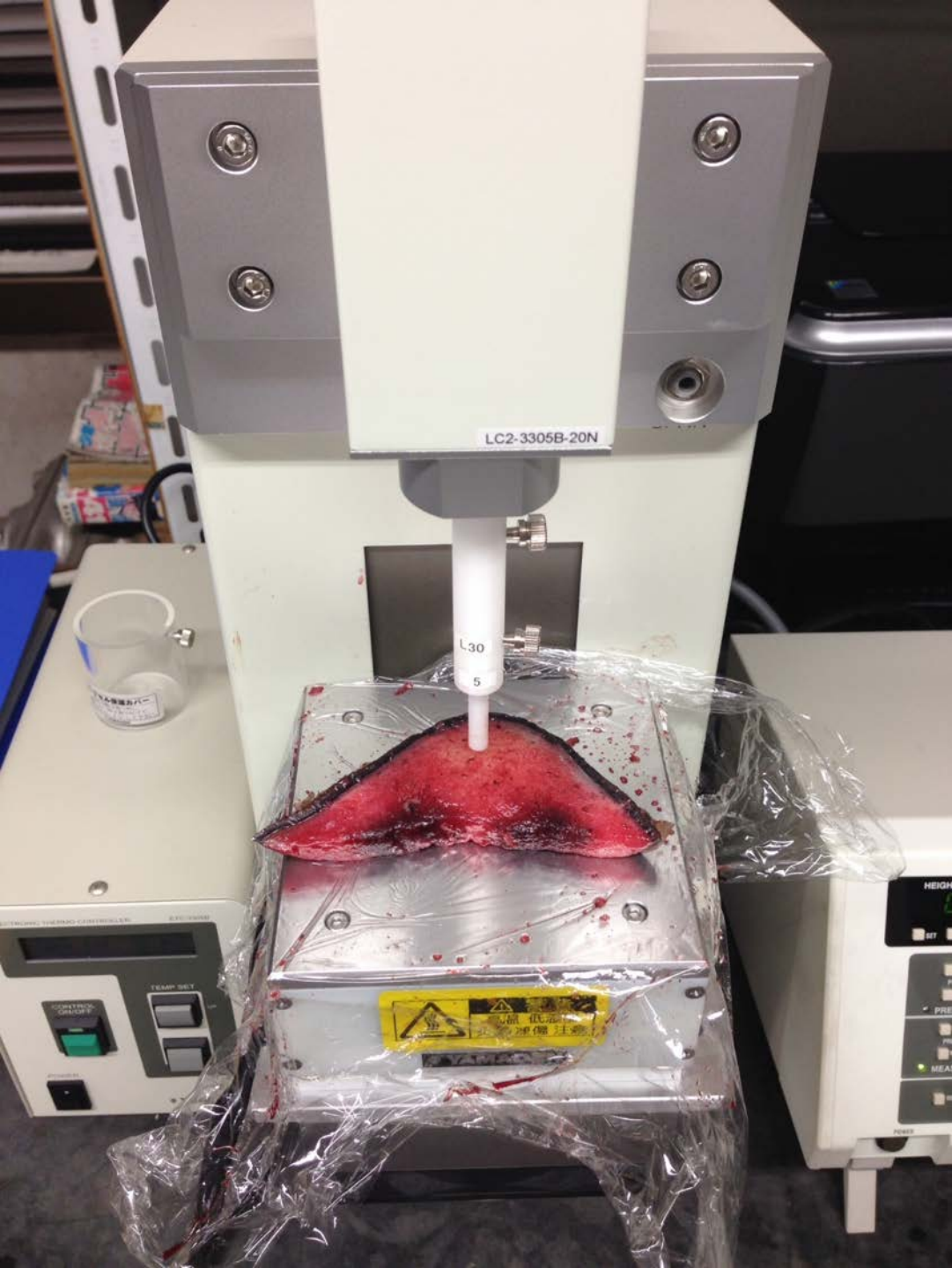
LC2-3305B-20N
30
5

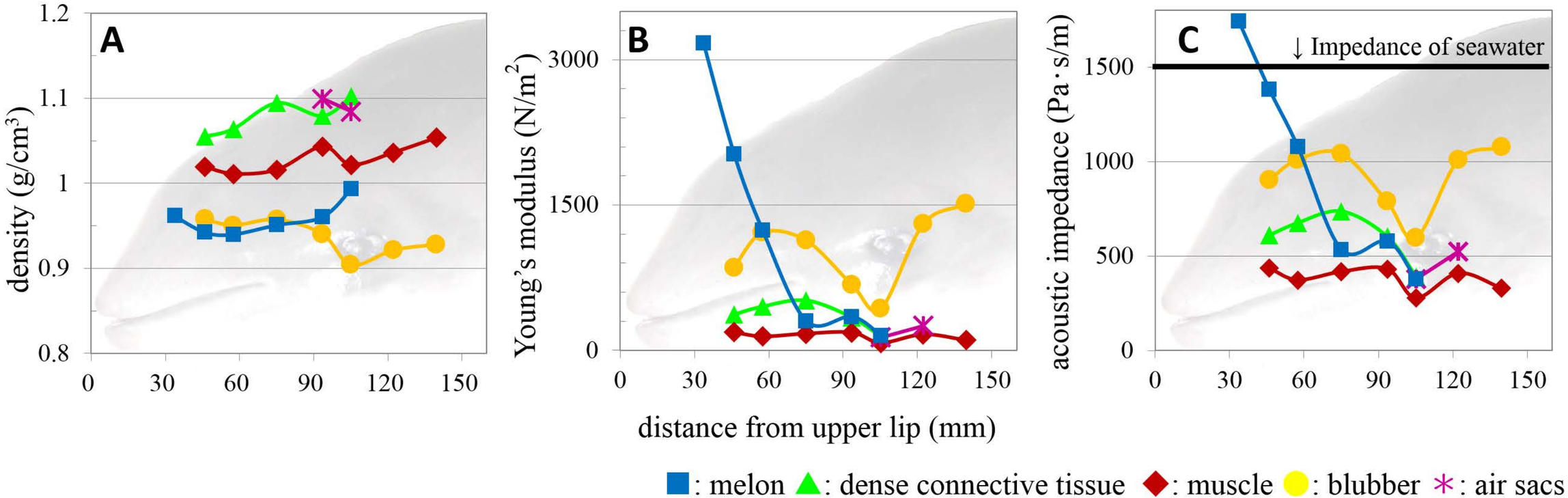
A
density (g/cm3)
1.2
1.1
1
0.9
0.8
0
30
60
90
120
150
B
Young's modulus (N/m2)
3000
1500
0
C
↓ Impedance of seawater
acoustic impedance (Pa·s/m)
1500
1000
500
0
distance from upper lip (mm)
: melon
: dense connective tissue
: muscle
: blubber
: air sacs

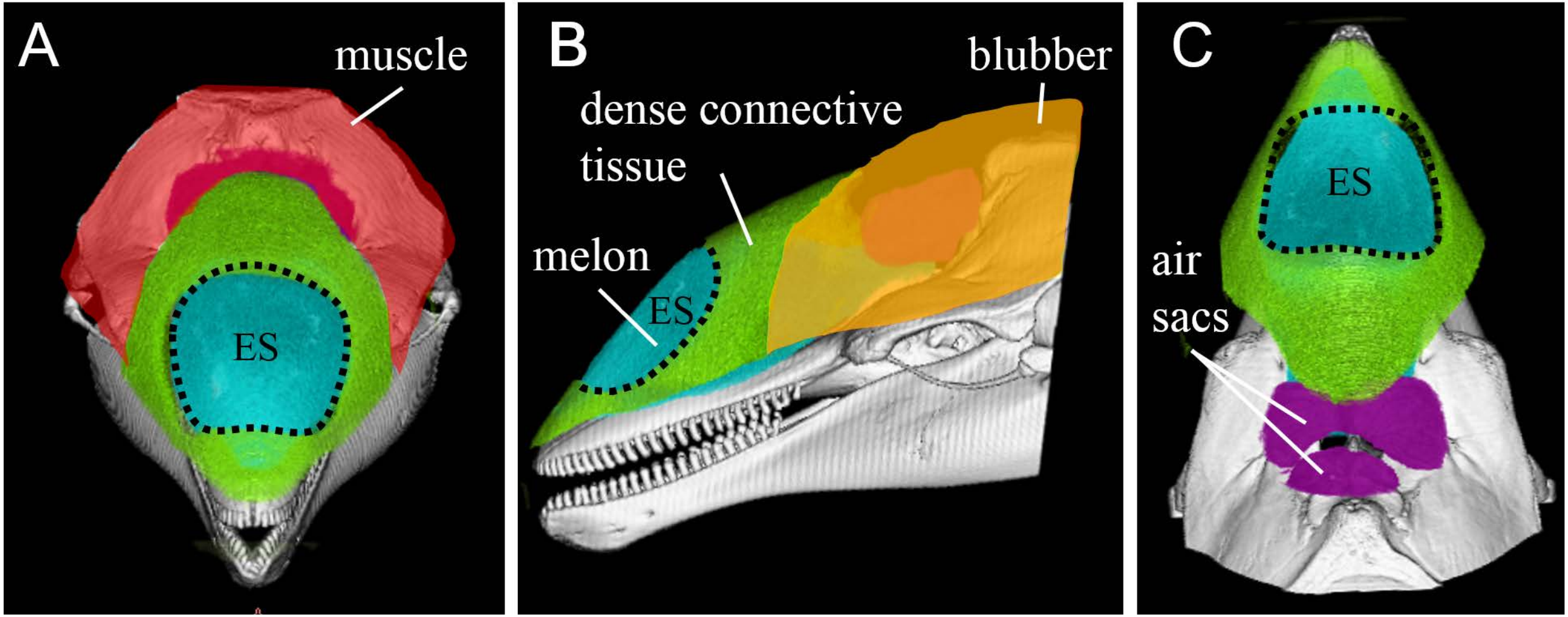
A
muscle
ES
B
blubber
dense connective
tissue
melon
ES
C
ES
air
sacs

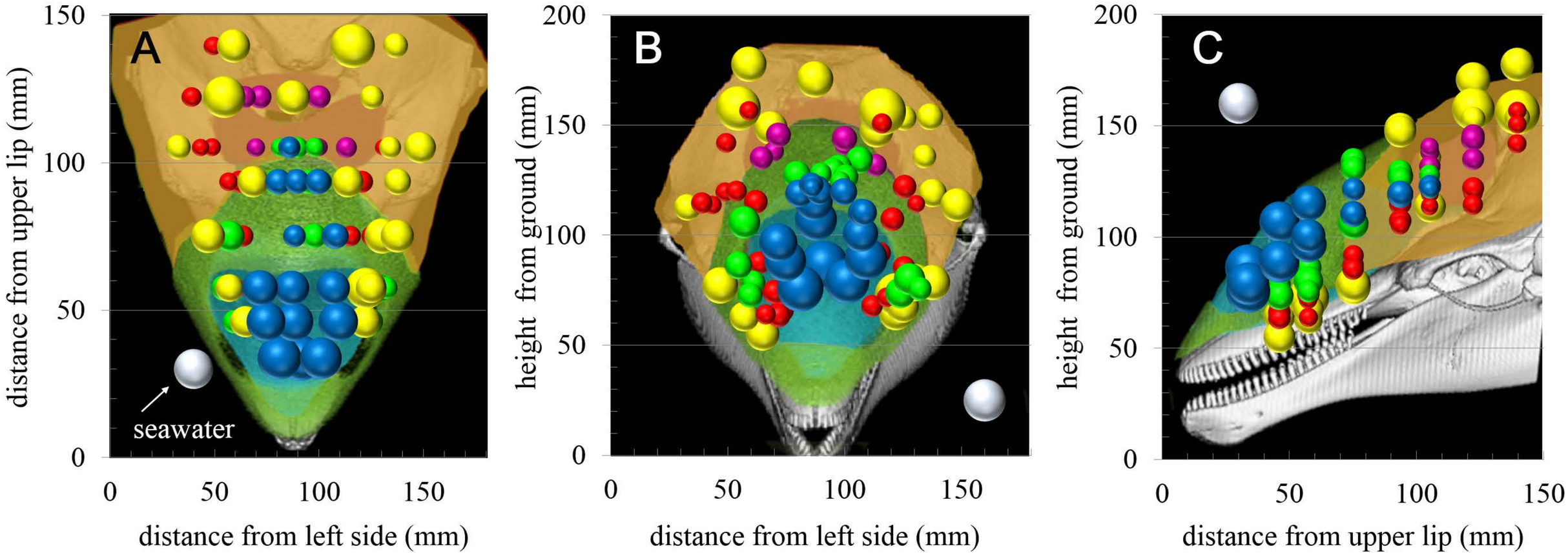
A
B
C
seawater
distance from upper lip (mm)
height from ground (mm)
distance from left side (mm)
0
50
100
150
200

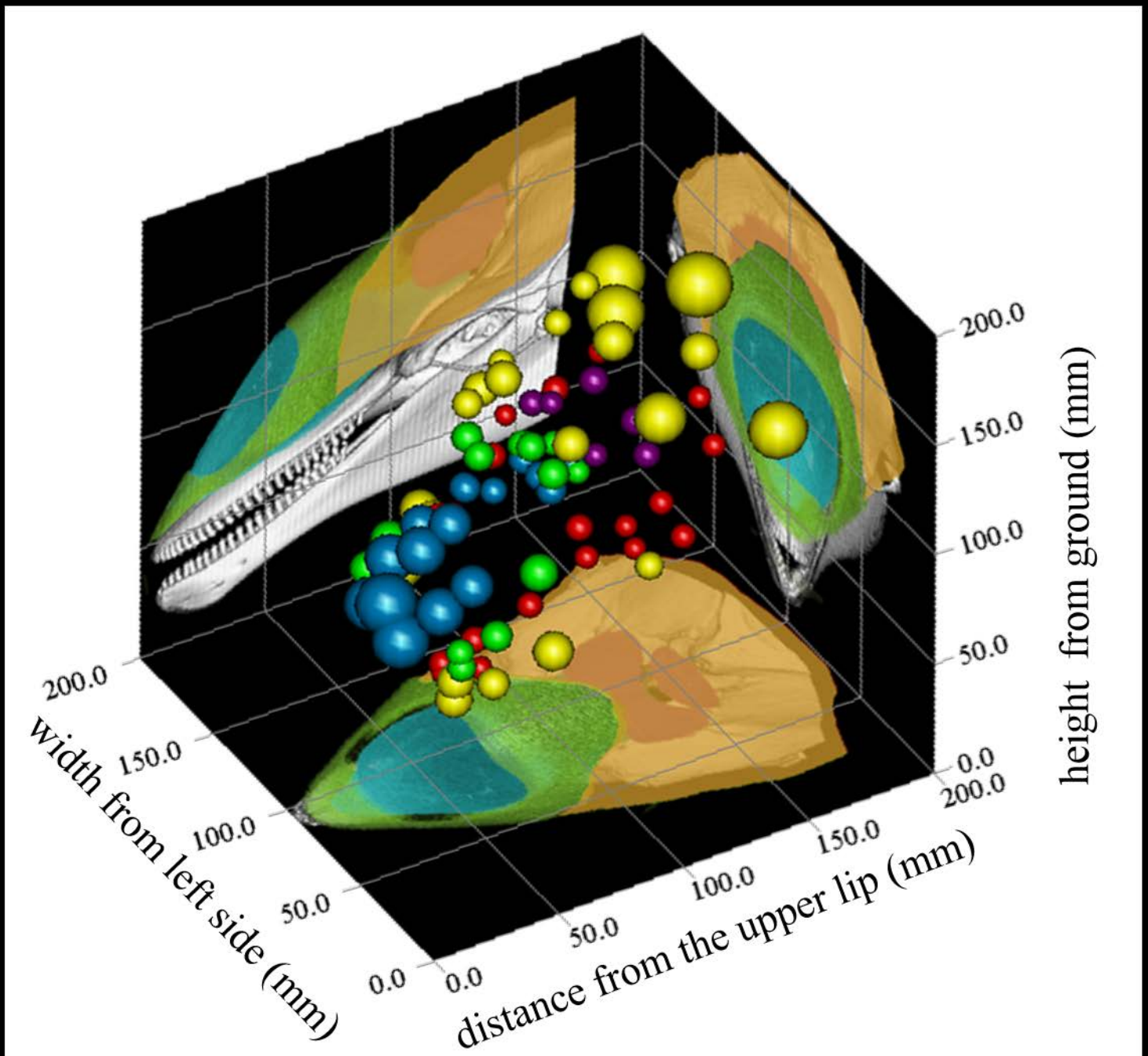
200.0
150.0
100.0
50.0
0.0
width from left side (mm)
0.0
50.0
100.0
150.0
200.0
distance from the upper lip (mm)
200.0
150.0
100.0
50.0
0.0
height from ground (mm)